

Original paper

# Whole-body diffusion-weighted imaging with background body signal suppression and quantitative apparent diffusion coefficient in the detection, staging, and grading of non-Hodgkin lymphoma

Ahmed A.K.A. Razeq<sup>1,A,C,D,E,F</sup>, Ahmed M. Tawfik<sup>1,A,D,E,F</sup>, Mariam Abdel Rahman<sup>1,B,C,E</sup>, Saleh Teima<sup>2,A,B,E</sup>,  
Nihal M Batouty<sup>1,B,C,D,E,F</sup>

<sup>1</sup>Department of Diagnostic and Interventional Radiology, Faculty of Medicine, Mansoura University, Mansoura, Egypt

<sup>2</sup>Department of Radiotherapy, Faculty of Medicine, Mansoura University, Mansoura, Egypt

## Abstract

**Purpose:** Assess reproducibility of detection, staging, and grading of non-Hodgkin lymphoma (NHL) using whole-body diffusion-weighted imaging with background body signal suppression (WB-DWIBS).

**Material and methods:** Thirty NHL patients underwent WB-DWIBS, divided into 2 groups according to staging and grading. Image analysis and apparent diffusion coefficient (ADC) measurement of the largest lymph node in each group were performed by 2 observers. Inter-observer agreement was performed.

**Results:** Overall inter-observer agreement for detection of NHL was excellent ( $\kappa = 0.843$ ; 92.05%) with excellent inter-observer agreement of nodal disease (cervical, thoracic and abdominal) ( $\kappa = 0.783, 0.769, \text{ and } 0.856$ ; 96.67%, 90.0%, and 93.3% respectively), extra-nodal disease ( $\kappa = 1$ ; 100%), and splenic involvement ( $\kappa = 0.67$ ; 83.3%). The overall inter-observer agreement of DWIBS in staging of NHL was excellent ( $\kappa = 0.90$ ; 94.9%) with excellent inter-observer agreement for stage I ( $\kappa = 0.93$ ; 96.4%), stage II ( $\kappa = 0.90$ ; 94.8%), stage III ( $\kappa = 0.89$ ; 94.6%), and stage IV ( $\kappa = 0.88$ ; 94.0%). There was significant difference between ADC in stage I, II ( $0.77 \pm 0.13, 0.85 \pm 0.09 \times 10^{-3} \text{ mm}^2/\text{s}$ ), and stage III, IV ( $0.63 \pm 0.08, 0.64 \pm 0.11 \times 10^{-3} \text{ mm}^2/\text{s}$ ,  $p < 0.002, < 0.001$ ). Interclass correlation showed almost perfect agreement for ADC measurement in staging and grading groups ( $r = 0.96$  and  $r = 0.85$ , respectively,  $p < 0.001$ ). There was significant difference between ADC in aggressive lymphoma ( $0.65 \pm 0.1, 0.67 \pm 0.13 \times 10^{-3} \text{ mm}^2/\text{s}$ ) and indolent lymphoma ( $0.76 \pm 0.14, 0.84 \pm 0.09 \times 10^{-3} \text{ mm}^2/\text{s}$ ,  $p < 0.028, < 0.001$ ).

**Conclusion:** DWIBS is reproducible for detection and staging of nodal and extra-nodal involvement in patients with NHL. ADC can quantitatively participate in the staging and grading of NHL.

**Key words:** non-Hodgkin lymphoma, whole body diffusion-weighted imaging with background suppression, magnetic resonance imaging, staging, grading, apparent diffusion coefficient.

## Introduction

Non-Hodgkin lymphoma (NHL) comprises a heterogeneous group of malignant diseases with high morbidity and mortality. The Lugano classification of lymphoma describes the extent of the disease detected by imaging for

the staging of lymphoma [1]. Imaging studies have played an important role in early diagnosis and accurate staging of lymphoma as well as evaluation of the treatment response. Contrast-enhanced computed tomography (CT) and conventional whole-body magnetic resonance imaging (MRI) are commonly used for the detection of disease

## Correspondence address:

Nihal M. Batouty, Department of Diagnostic and Interventional Radiology, Faculty of Medicine, Mansoura University, 60 El Gomhouria St, Mansoura, Dakahlia, Egypt, e-mail: [nihalbatouty@gmail.com](mailto:nihalbatouty@gmail.com)

## Authors' contribution:

A Study design · B Data collection · C Statistical analysis · D Data interpretation · E Manuscript preparation · F Literature search · G Funds collection

sites and monitoring of the morphological changes after treatment. However, they rely on the size criterion and could not differentiate between malignant and benign lesions. Fluorodeoxyglucose positron emission CT (FDG-PET-CT) could differentiate aggressive from indolent lymphoma and guide biopsies requested for the detection of histological transformation of indolent lymphoma. However, it is expensive, time-consuming, and involves exposure to ionizing radiation [2,3].

Many studies have demonstrated the feasibility and reliability of whole-body CT and MRI, especially with diffusion-weighted imaging (DWI), as an alternative tool for staging of lymphoma, determination of tumour burden, prognostic biomarker, and assessment of treatment response [4-7]. Quantitative assessment of lymphoma was carried out in previous studies using apparent diffusion coefficient (ADC) measurement. They investigated nodal characterization in paediatric Hodgkin lymphoma patients and differentiation between normal, benign, malignant, and lymphomatous lymph nodes [8-10]. The advantage of whole-body MRI over PET/CT is being a non-irradiating imaging tool with no need for radioisotope or intravenous contrast. Additionally, whole body MRI has lower cost and faster acquisition time [3,11-21].

Whole-body MRI covers a large field of view (FOV) in a single examination and enables multi-region scanning [15]. Various obstacles initially limited the usefulness of whole-body MRI with 3-T MRI machines, such as magnetic susceptibility artifacts, the signal-to-noise ratio (SNR) which is doubled in 3.0 T, and geometrical distortions, but these problems have been resolved, and now whole-body MRI is technically feasible with both 1.5-T and 3-T scanners [15]. Whole-body protocols have evolved since they were first used 2 decades ago. Now it combines optimal anatomical information from 2 anatomical sequences: T1-weighted and short time inversion recovery (STIR), while functional qualitative and quantitative data, including DWI with ADC measurement, provide useful information from multiple regions of the body [7,15].

Diffusion-weighted magnetic resonance imaging probes the random Brownian motion of water molecules in the body. Lymphomas have relatively high signal intensity on DWI compared to normal tissues because of their high

cellularity and elevated nuclear-to-cytoplasm ratio [22]. DWI has been considered an imaging modality that provides both morphological and functional information regarding characterization of lymphomas, and it has been used for the detecting and staging of malignant lymphomas, as well as for monitoring the response to therapy [4,7,23-28]. DWI requires breath holding or respiratory triggered scanning for imaging the visceral (moving) organs, because the respiratory motion is markedly larger than diffusion, which was believed to cause loss of diffusion-weighted image contrast [4,29].

The concept of DWI with background body signal suppression (DWIBS) was firstly introduced by Takahara *et al.* in 2004 as a technique for whole-body DWI that acquires diffusion data from visceral (moving organs) during free breathing. Background suppression improves the contrast between the lesions and normal tissues, which allows better detection of lesions. The feasibility of free breathing with DWIBS could be explained by understanding 2 types of motion: intravoxel incoherent and intravoxel coherent. Diffusion means incoherent motion of water molecules within a voxel, while coherent motion of water molecules within a voxel refers to the respiratory motion [30]. The advantage of DWIBS over anatomical MRI or CT is that small lesions may be obscured or overlooked in conventional MRI or CT due to the large amount of image data or the presence of lesions in normal-sized organs [30].

The aim of this study is to assess the reproducibility of detection, staging, and grading of NHL using WB-DWIBS.

## Material and methods

### Patients

Institutional Review Board approval and informed consent from all the patients were obtained. Inclusion criteria for participation in this study were age above 18 years, newly diagnosed NHL and referred for staging, biopsied, and with pathologically proven NHL. All patients underwent whole body T1WI, DWIBS, and STIR as a fat suppression sequence. Histopathological diagnosis and determination of subtypes were done according to the criteria of the current WHO classification of haematological and lymphoid malignancies [31].

### Technique

Whole-body MRI was performed using a 1.5-Tesla machine (Ingenia, Philips healthcare, Best, Netherlands). The scan time was about 25-35 minutes. Whole-body coronal non-fat saturated TIWI, STIR, and coronal and axial DWIBS images were obtained for 7 separate sites: 1) head, neck, chest apex, proximal upper limb, and cervical spine; 2) chest, upper abdomen, upper limb, dorsal, and upper lumbar spine; 3) lower abdomen and upper pelvis; 4) lower pelvis and thighs; 5) distal femora, knee joint, and

**Table 1.** The imaging parameters used for whole-body MRI T1WI, STIR, and DWIBS sequences

	T1WI	STIR	DWIBS
TR (repetition time)	400 ms	3000-5000 ms	7410 ms
TE (echo time)	4 ms	70 ms	60 ms
Ti (inversion time)	-	165 ms	165 ms
Slice thickness	6 mm	6 mm	3 mm
FOV	300-360 mm	300-360 mm	250 mm
Matrix	256 × 256	256 × 256	256 × 256
b-value	-	-	1000

proximal both tibiae; 6) tibia and fibula; 7) distal tibia, distal fibula, and foot. DWIBS images were obtained during free breathing. The imaging parameters used for T1WI, STIR, and DWIBS sequences are demonstrated in Table 1.

Merging of the images was performed at multiple anatomical positions of the whole body of each sequence into the coronal plane. The whole-body image reconstruction was done by multi-planar reformats. Inversion of the greyscale of DWIBS images was done.

### Image analysis

Image analysis was performed using a Philips workstation with commercially available software. Two radiologists (AT, NB) with experience of 16 and 10 years, respectively, in MRI imaging, who were blinded to the clinical findings and pathological diagnosis, independently reviewed axial and coronal WB-DWIBS images.

Image analysis was performed for nodal and extra-nodal involvement in different regions of the body according to Lugano classification for staging and response assessment of lymphomas [32]. Staging was done based on the extent of involvement of nodal groups, as follows: stage I, single lymph node group; stage II, multiple lymph node groups ipsilateral to the diaphragm; stage III, involvement of lymph node groups both above and below the diaphragm; and stage IV, non-contiguous extra nodal involvement (e.g. liver, lung, or bone marrow). Lymph node involvement was considered positive when larger than 10 mm in its longest transverse diameter, except for those with a clearly identified fatty hilum and thin cortex [33]. For 2 regions, axillary and femoral, the significant size was larger than 15 mm. Image analysis was performed for 16 regions (cervical, supraclavicular, internal mammary and diaphragmatic, anterior mediastinal, para-tracheal, hilar, sub-carinal and posterior mediastinal, celiac and superior mesenteric, hepatic and splenic hilar, retroperitoneal and peri-aortic, and inferior mesenteric lymph nodes). The lymph node signal intensity was visually assessed. For ADC extraction by both observers, a region of interest (ROI) was manually drawn to contour the whole largest lymph node of each group (cervical, thoracic, and abdominal) at the largest section, and then the average value of all readings was calculated for each patient.

### Statistical analysis

Data were analysed using the Statistical Package for the Social Sciences, version 22 (SPSS Inc., Chicago, IL, USA). Quantitative data were described using mean and standard deviation. After testing normality using the Kolmogorov-Smirnov test, Student's *t*-test was used to compare stage I, II and stage III, IV of lymphoma, and to compare aggressive and indolent lymphomas. Receiver operating characteristic (ROC) curve analysis was used to test the diagnostic performance and accuracy of ADC to differentiate be-

tween stage I, II and stage III, IV of lymphoma, and between aggressive and indolent lymphomas. Sensitivity and specificity were detected from the curve and PPV, NPV, and accuracy were calculated through cross tabulation. The inter-observer agreement was assessed by kappa ( $\kappa$ ) statistic with 95% confidence intervals (CI); the  $\kappa$  coefficient is the amount of observed agreement. A  $\kappa$  of 1.0 represents perfect agreement, a  $\kappa$  of 0.81 to 1.0 is excellent agreement, and a  $\kappa$  of 0.61 to 0.80 is good agreement. Interclass correlation (ICC) was run to test the inter-observer agreement for continuous data by calculating *r*, which is interpreted as follows: 0.5-0.6 moderate agreement, 0.7-0.8 strong agreement, and > 0.8 almost perfect agreement. *P*-value < 0.05 was considered statistically significant.

## Results

### Demographics

This prospective study was carried out on 31 consecutive patients with NHL. One patient was excluded from the study due to bad quality of DWIBS images caused by motion artifacts; a total of 30 patients were included. They were 17 males and 13 females with mean age 46 years, range (18-69 years). Patients were presented with enlarged cervical lymph nodes (*n* = 26), cachexia (*n* = 22), and easy fatigability (*n* = 29). Final histopathological diagnosis was 30 patients with NHL as follows: diffuse large B-cell lymphoma (DLBCL) in 17 patients, small B-cell lymphoma in 12 patients (follicular lymphoma in 6 patients, chronic lymphocytic leukaemia in 3 patients and marginal zone lymphoma in 3 patients), and Burkitt's lymphoma in one patient. Patients were categorized according to the stage of lymphoma into 2 groups: stage I, II (*n* = 12) and stage III, IV (*n* = 18), and according to the grade of lymphoma into aggressive lymphoma (DLBCL, Burkitt's lymphoma) (*n* = 18) and indolent lymphoma (small B-cell lymphoma) (*n* = 12).

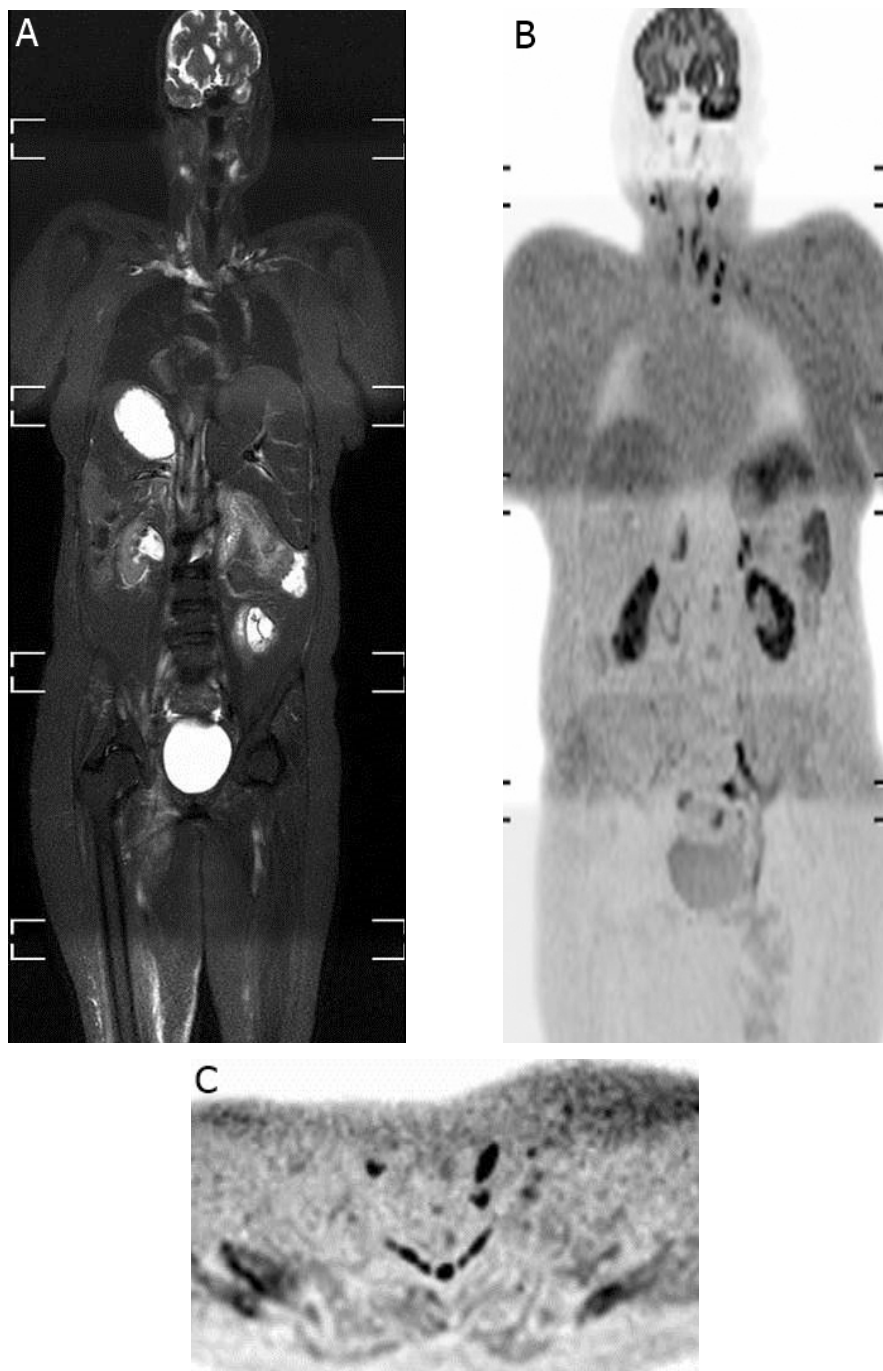
### Detection

Table 2 shows the inter-observer agreement of DWIBS in the detection of nodal, extra-nodal, and spleen of NHL. The overall inter-observer agreement of lymphoma detection over the whole body was excellent ( $\kappa$  = 0.8; 92%).

Nodal lymphomas (Figures 1-3): cervical lymph node involvement was reported in 27 patients by observer 1 and in 28 patients by observer 2. The overall inter-observer agreement of DWIBS in diagnosis was excellent ( $\kappa$  = 0.78; 97%). Thoracic lymph node involvement was reported in 22 patients by observer 1 and in 21 patients by observer 2. The overall inter-observer agreement of DWIBS in diagnosis was excellent ( $\kappa$  = 0.77, 90%). Abdominal lymph node involvement was reported in 19 patients by observer 1 and in 19 patients by observer 2. The overall inter-observer agreement of DWIBS in diagnosis was excellent ( $\kappa$  = 0.86; 93%). Extranodal lymphomas (bony [spinal, ap-

**Table 2.** Inter-observer agreement of DWIBS in the detection of nodal, extra nodal, and spleen in patients with NHL

	Observer 1	Observer 2	Percentage agreement	$\kappa$	95% CI	<i>p</i> -value
<b>Nodal</b>						
Cervical	27 (90%)	28 (93%)	97%	0.78	0.4-1	< 0.001*
Thoracic	20 (67%)	21 (70%)	90%	0.77	0.5-1	< 0.001*
Abdominal	19 (63%)	19 (63%)	93%	0.86	0.7-1	< 0.001*
Extra nodal	12 (100%)	12 (100%)	100%	1	1-1	< 0.001*
Spleen	16 (53%)	15 (50%)	83%	0.67	0.4-0.9	< 0.001*
Overall	94 (63%)	95 (63%)	92%	0.84	0.7-0.9	< 0.001*



**Figure 1.** Whole-body magnetic resonance imaging of non-Hodgkin lymphoma, stage I. A) Coronal STIR whole-body image shows enlarged cervical lymph nodes with high signal intensity. B) Coronal diffusion-weighted imaging with background body signal suppression (DWIBS) whole-body image shows restricted diffusion of the lesion. C) Axial neck DWIBS image shows enlarged cervical lymph nodes with restricted diffusion

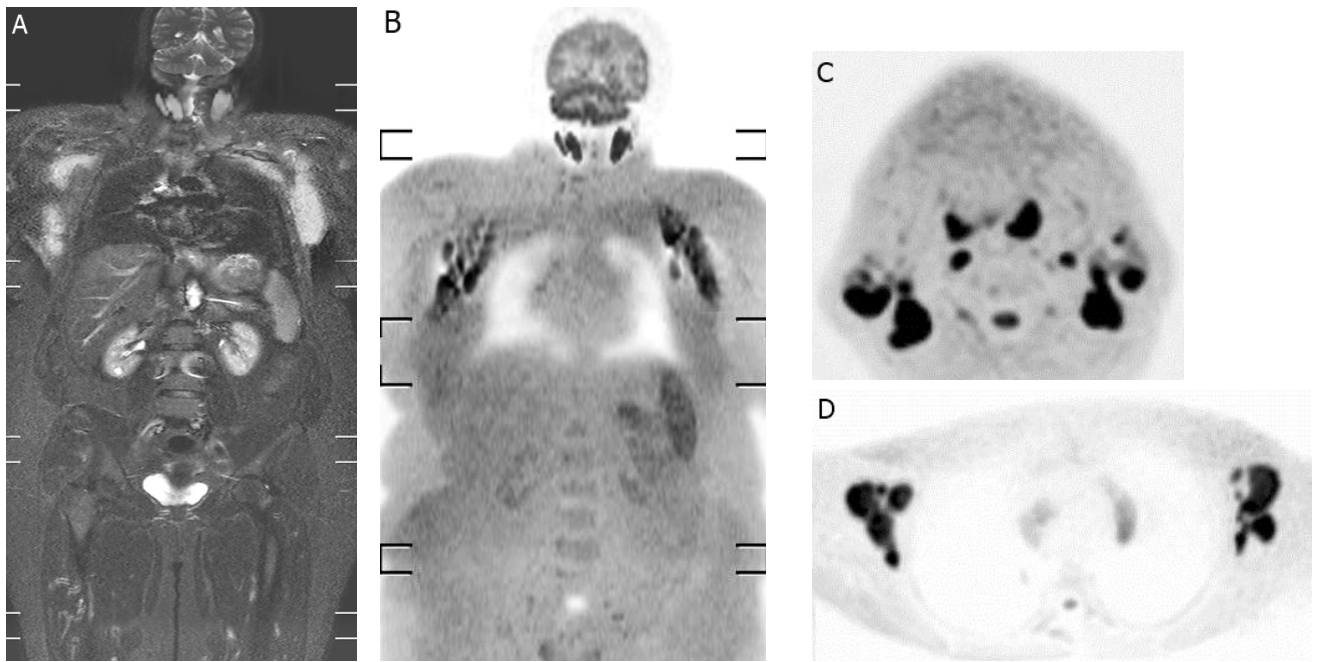


**Figure 2.** Whole-body magnetic resonance imaging of non-Hodgkin lymphoma, stage II. **A)** Coronal STIR whole-body image shows enlarged cervical and axillary lymph nodes with high signal intensity. **B)** Coronal diffusion-weighted imaging with background body signal suppression (DWIBS) whole-body image shows restricted diffusion of the lesions. **C)** Axial neck DWIBS image shows enlarged cervical lymph nodes with restricted diffusion. **D)** Axial chest DWIBS image shows enlarged axillary lymph nodes with restricted diffusion

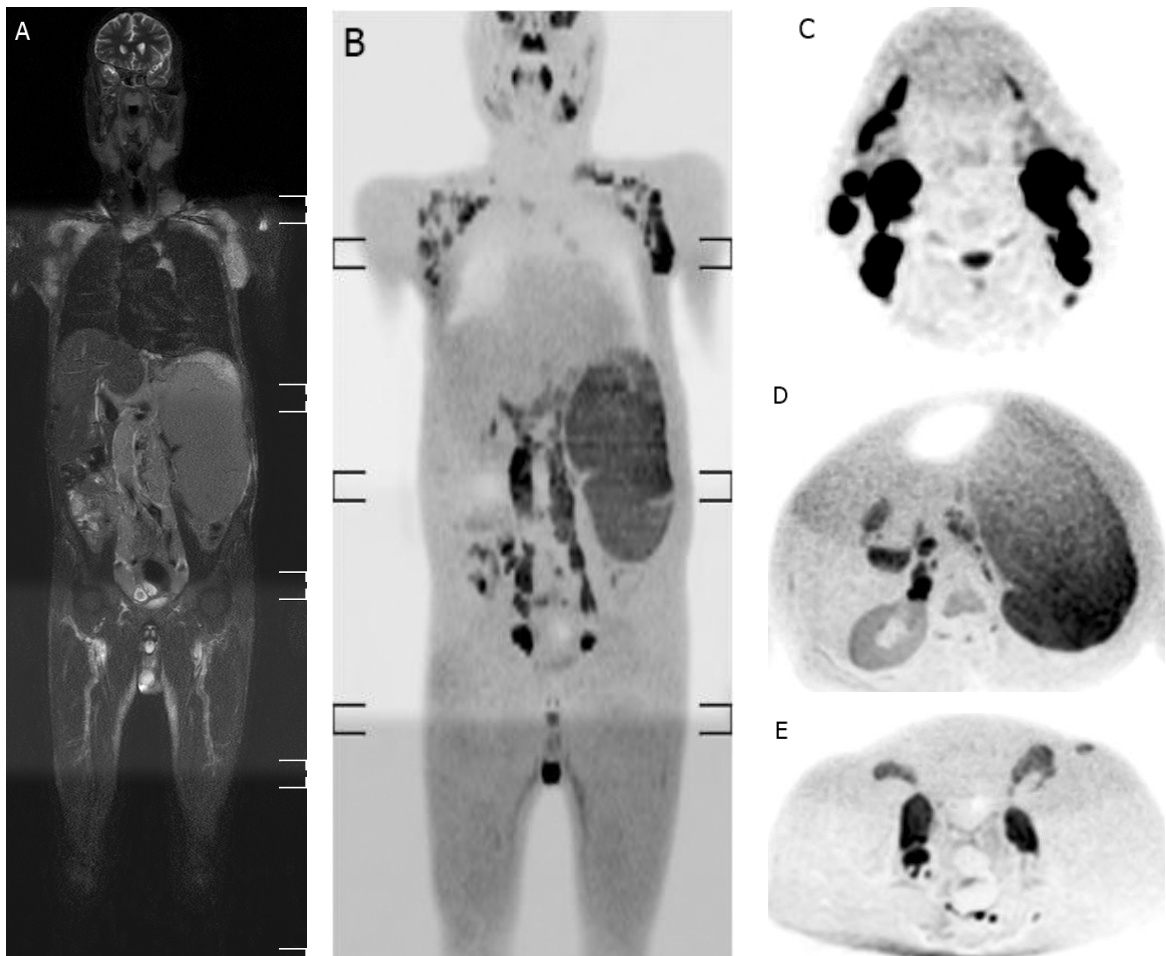


**Figure 3.** Whole-body magnetic resonance imaging of non-Hodgkin lymphoma, stage III. **A)** Coronal STIR whole-body image shows hyperintense enlarged right parotid, bilateral cervical, supraclavicular, infraclavicular, axillary, porta hepatis, paraaortic and iliac lymph nodes; some of them form masses of amalgamated lymph nodes; the largest is located at the left iliac region; also note the diffuse parenchymal infiltration of the spleen. **B)** Coronal diffusion-weighted imaging with background body signal suppression (DWIBS) whole-body image shows restricted diffusion of the lesions. **C)** Axial neck DWIBS image shows restricted diffusion of right parotid and bilateral cervical lymph nodes. **D)** Axial abdomen DWIBS image shows splenic infiltration with multiple enlarged porta hepatis lymph node with restricted diffusion. **E)** Axial pelvis DWIBS image shows bilateral enlarged iliac lymph nodes with right iliac nodal mass of amalgamated lymph nodes with restricted diffusion

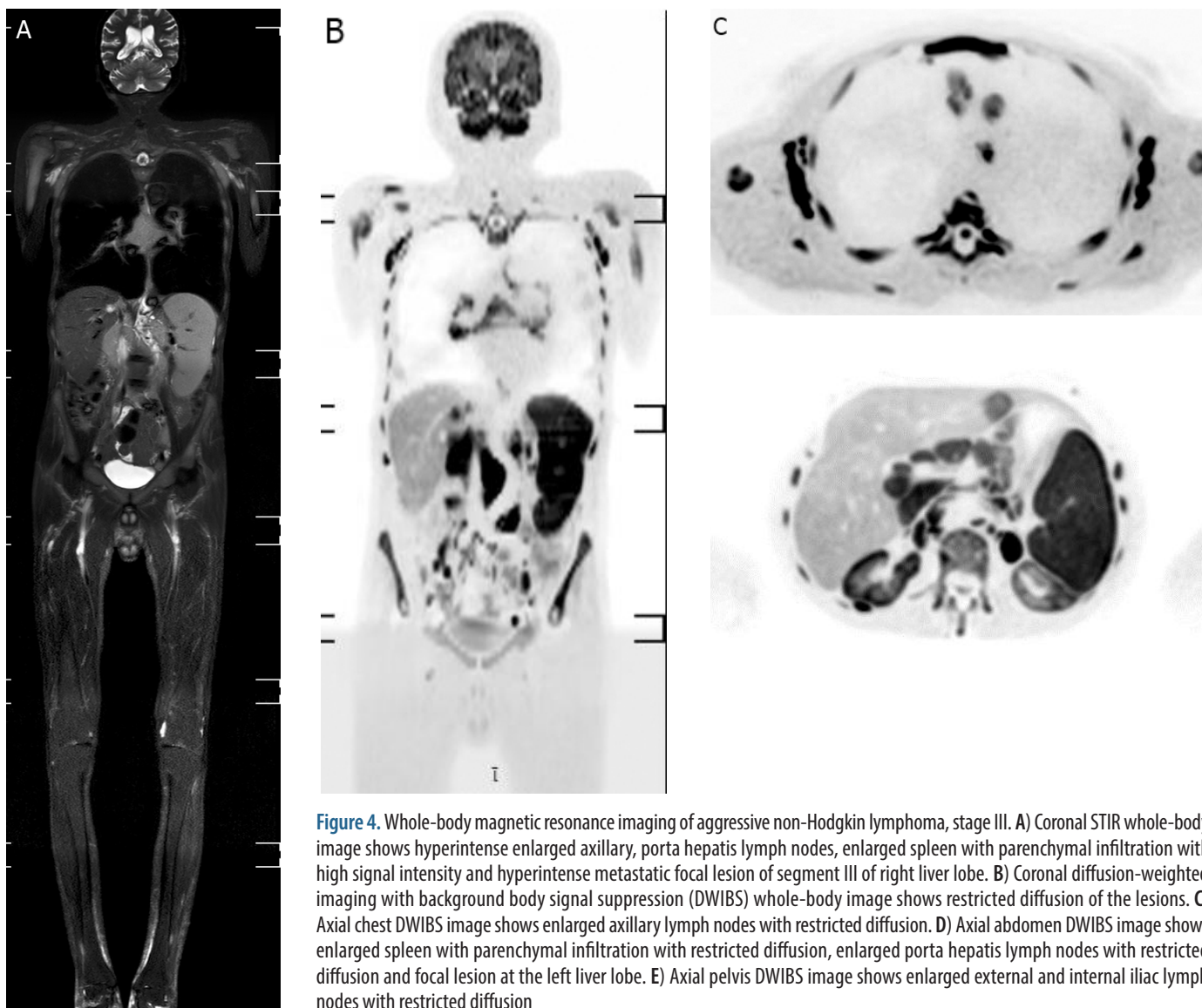


**Figure 4.** Whole-body magnetic resonance imaging of aggressive non-Hodgkin lymphoma, stage III. A) Coronal STIR whole-body image shows hyperintense enlarged axillary, porta hepatis lymph nodes, enlarged spleen with parenchymal infiltration with high signal intensity and hyperintense metastatic focal lesion of segment III of right liver lobe. B) Coronal diffusion-weighted imaging with background body signal suppression (DWIBS) whole-body image shows restricted diffusion of the lesions. C) Axial chest DWIBS image shows enlarged axillary lymph nodes with restricted diffusion. D) Axial abdomen DWIBS image shows enlarged spleen with parenchymal infiltration with restricted diffusion, enlarged porta hepatis lymph nodes with restricted diffusion and focal lesion at the left liver lobe. E) Axial pelvis DWIBS image shows enlarged external and internal iliac lymph nodes with restricted diffusion

pendicular], hepatic, pulmonary, and peritoneal) (Figure 4) was reported in 12 patients by observer 1 and in 12 patients by observer 2, with excellent agreement ( $\kappa = 1$ ; 100%). Splenic lymphoma (Figure 4) was reported in 16 patients by observer 1 and in 15 patients by observer 2, with excellent agreement ( $\kappa = 0.67$ ; 83%).

### Staging

Stage I lymphoma was reported in 4 patients by both observers, with excellent agreement ( $\kappa = 0.71$ ; 93%). Stage II lymphomas were reported in 8 and 10 patients observer 1 and 2, respectively, with excellent agreement ( $\kappa = 0.6$ ; 87%). Stage III was reported in 12 and 10 patients by observer 1 and 2, respectively, with excellent agreement ( $\kappa = 0.8$ ; 93%). Stage IV was reported in 6 patients by both observers with excellent agreement ( $\kappa = 1$ ; 100%). The overall inter-observer agreement of WBMRI in staging of lymphoma was excellent ( $\kappa = 0.82$ ; 87%) (Table 3). The mean

ADC of patients with stage I, II lymphoma ( $0.77 \pm 0.13 \times 10^{-3}$ ,  $0.85 \pm 0.09 \times 10^{-3}$  mm<sup>2</sup>/s) was significantly different ( $p < 0.002$ ,  $< 0.001$ ) from patients with stage III, IV ( $0.63 \pm 0.08 \times 10^{-3}$ ,  $0.64 \pm 0.11 \times 10^{-3}$  mm<sup>2</sup>/s for observer 1 and 2, respectively). The cut-off ADC value that differentiates between stage I, II and stage III, IV lymphoma patients was  $0.77 \times 10^{-3}$ ,  $0.72 \times 10^{-3}$  mm<sup>2</sup>/s; the best results were obtained with AUC 0.86, 0.93, accuracy 83% for both, sensitivity 94%, 82%, specificity 69%, 85%, PPV 80%, 88%, and NPV 90%, 79% for observer 1 and 2 respectively. ICC showed almost perfect agreement between both observers ( $r = 0.96$ ,  $p < 0.001$ ) (Table 4 and 5, Figure 5).

### Grading of lymphoma

The mean ADC of patients with aggressive lymphoma ( $0.65 \pm 0.1$ ,  $0.67 \pm 0.13 \times 10^{-3}$  mm<sup>2</sup>/s) was significantly different ( $p < 0.028$ ,  $< 0.001$ ) from patients with indolent lymphoma ( $0.76 \pm 0.14$ ,  $0.84 \pm 0.09 \times 10^{-3}$  mm<sup>2</sup>/s for ob-

**Table 3.** Inter-observer agreement of staging of non-Hodgkin lymphoma

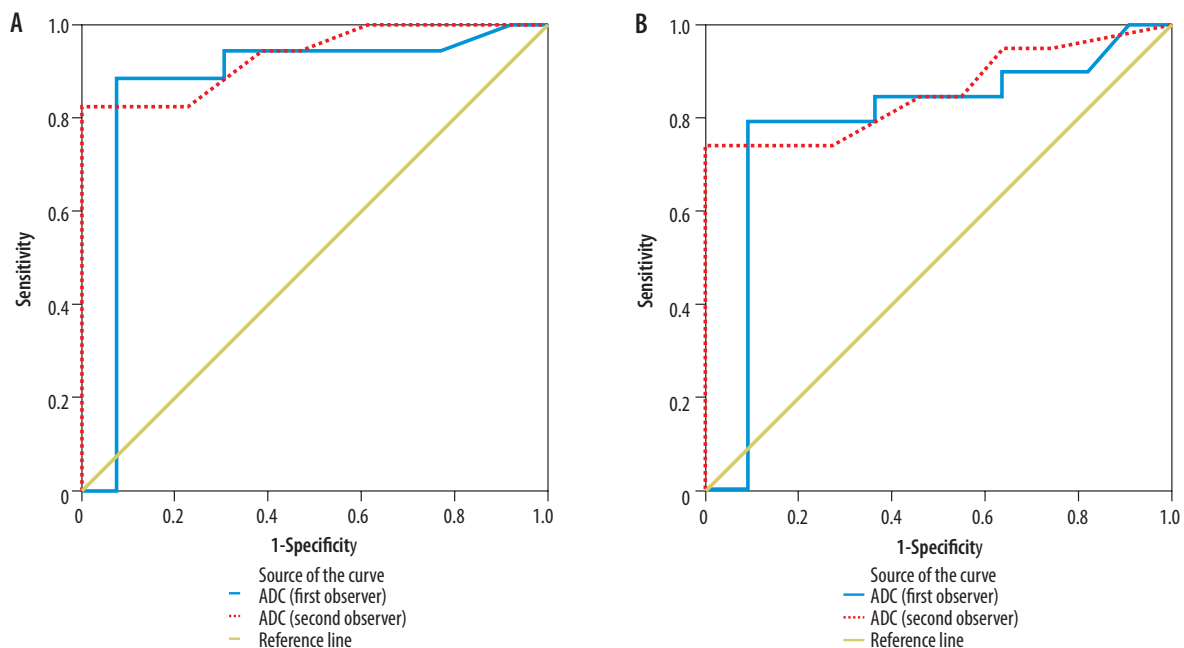
Stage	Observer 1	Observer 2	Percentage agreement	$\kappa$	95% CI	<i>p</i> -value
Stage I	4 (13%)	4 (13%)	93%	0.71	0.3-1.0	<0.001*
Stage II	8 (27%)	10 (33%)	87%	0.68	0.4-0.9	<0.001*
Stage III	12 (40%)	10 (33%)	93%	0.86	0.7-1.0	<0.001*
Stage IV	6 (20%)	6 (20%)	100%	1.00	1.0-1.0	<0.001*
Overall	30 (100%)	30 (100%)	87%	0.82	0.7-0.9	<0.001*

**Table 4.** Inter-observer agreement of grading of non-Hodgkin lymphoma (NHL), mean and SD of ADC of staging and grading of NHL

	Observer 1; mean $\pm$ SD $\times 10^{-3}$ mm <sup>2</sup> /s	Observer 2, mean $\pm$ SD $\times 10^{-3}$ mm <sup>2</sup> /s	<i>p</i> -value
<b>Staging</b>			
Stage I-II ( <i>n</i> = 12)	0.77 $\pm$ 0.13	0.85 $\pm$ 0.09	< 0.002*
Stage III-IV ( <i>n</i> = 18)	0.63 $\pm$ 0.08	0.64 $\pm$ 0.11	< 0.001*
<b>Grading</b>			
Aggressive ( <i>n</i> = 18)	0.65 $\pm$ 0.1	0.67 $\pm$ 0.13	< 0.028*
Agreement	<i>r</i> = 0.852		< 0.001*
Indolent ( <i>n</i> = 12)	0.76 $\pm$ 0.14	0.84 $\pm$ 0.09	< 0.001*
Agreement	<i>r</i> = 0.869		< 0.001*

**Table 5.** ROC curves to differentiate between low and high stages and aggressive from indolent lymphoma patients

	AUC (95%CI)	<i>p</i> -value	Cut-off point	Sensitivity (%)	Specificity (%)	PPV (%)	NPV (%)	Accuracy (%)
<b>Staging</b>								
ADC (Observer 1)	0.86	0.001*	$0.77 \times 10^{-3}$ mm <sup>2</sup> /s	94	69	80	90	83
ADC (Observer 2)	0.93	0.001*	$0.72 \times 10^{-3}$ mm <sup>2</sup> /s	82	85	88	79	83
<b>Grading</b>								
ADC (Observer 1)	0.79	0.01*	$0.77 \times 10^{-3}$ mm <sup>2</sup> /s	84	64	80	70	77
ADC (Observer 2)	0.85	0.001*	$0.72 \times 10^{-3}$ mm <sup>2</sup> /s	74	82	88	64	77

**Figure 5.** ROC curves in staging and grading of non-Hodgkin lymphoma. **A)** The cut-off value that differentiates stages I, II from stages III, IV was  $0.77 \times 10^{-3}$ ,  $0.72 \times 10^{-3}$  mm<sup>2</sup>/s, AUC 0.86, 0.93 for observer 1 and 2, respectively, and accuracy 83% for both. **B)** The cut-off value that differentiates aggressive from indolent lymphoma was  $0.77 \times 10^{-3}$ ,  $0.72 \times 10^{-3}$  mm<sup>2</sup>/s, AUC 0.79, 0.85 for observer 1 and 2, respectively, and accuracy 77% for both

server 1 and 2, respectively). The cut-off ADC value that differentiates between aggressive and indolent lymphoma patients was  $0.77 \times 10^{-3}$ ,  $0.72 \times 10^{-3}$  mm<sup>2</sup>/s; the best results were obtained with AUC 0.79, 0.85, accuracy 77% for both, sensitivity 84%, 74%, specificity 84%, 74%, PPV 80%, 88%, and NPV 70%, 64% for observer 1 and 2, respectively. ICC showed almost perfect agreement between both observers in both aggressive and indolent lymphoma ( $r = 0.85$  and  $r = 0.86$ ,  $p < 0.001$ ) (Table 4, Table 5, Figure 5).

## Discussion

WB-MRI including DWIBS and ADC measurement was used in patients with malignant NHL for detection, staging, and grading of nodal, splenic, and extra-nodal involvement in different regions of the whole body within a short examination time. The main finding in this study is that there is excellent inter-observer agreement of DWIBS in the detection of malignant lymphoma. ADC measurement showed high accuracy in the differentiation between stages I, II and stages III, IV lymphoma patients and between aggressive and indolent lymphoma patients.

DWIBS has the potential to become an important biomarker in oncology and is considered a reasonable substitute for PET/CT and CT. As recommended by as low as reasonably achievable (ALARA) principles, there is a need to minimize ionizing radiation in younger patients treated with curable potential [15]. WB-MRI with DWIBS has many advantages: it allows faster interpretation and easier visual assessment with the images reconstructed from multiple planes. This technique is acquired during free breathing; thus, it enables acquisition of thin axial sections, multiple signal averaging, and fat-suppression, which further enhances the regions of restricted diffusion [34-36]. The faster acquisition, lack of radiation, contrast medium, or isotope makes WB-DWIBS best suitable for screening in oncologic patients for staging then for repeated follow-up [37].

WB-MRI has been recommended as the reference imaging tool for staging and detection of tumour burden in lymphoma [38]. Nodal involvement was assessed by WB-MRI in several studies [9,10]. We had excellent inter-observer agreement of WB-MRI using DWIBS in the detection of cervical, thoracic, and abdominal lymph node involvement. Another study reported moderate-to-good inter-observer agreement of whole-body MRI-DWI for all nodal regions together and on individual regions except for the hilar lymph node region, which represented poor agreement [8]. Another study also added FDG-PET-CT to whole-body MRI-DWI for the evaluation of lymph node regions, with combined lymph node size and ADC analysis, DWIBS and PET/CT results showed excellent agreement, and high sensitivity and specificity [12]. WB-MRI including DWIBS is useful in the evaluation of extra-nodal lymphoma, DWIBS was better than PET-CT in detection of bone marrow involvement, while PET-CT was

better in pulmonary involvement in a previous study [12]. Concerning the reliability of WB-MRI in the detection of lymphomatous infiltration of the spleen, we found excellent agreement between both reviewers for the assessment of splenic involvement in malignant lymphoma. As regards splenic involvement in lymphoma patients using both FDG-PET/CT and WB-MRI, a sensitivity of 100% in WB-MRI was found in a previous study by Albano *et al.* [12].

Accurate staging of lymphoma is a crucial preliminary step for appropriate treatment planning and prediction of prognosis [38]. Previous studies demonstrated the reliability of WB-MRI, especially with DWI, as an alternative tool for staging of lymphoma, determination of tumour burden, prognostic biomarker, and assessment of treatment response [38-40]. This study shows that whole-body DWIBS can be used to stage patients with malignant lymphoma from size-based analysis of lymph node and ADC measurement. Previous studies reported excellent agreement between DWIBS and PET/CT as regards both lymph node and organ involvement [40,41]. DWIBS reflects tissue structure and cellularity, and may be complementary to FDG-PET, which indicates glucose metabolic activity and disease aggressiveness, but this relationship must be evaluated in further studies. Several studies have demonstrated the potential of whole-body DWIBS for lesion detection in oncology patients. Initial staging using WB-MRI (including T1- and T2-weighted images and DWIBS) equalled staging using contrast-enhanced MDCT [41]. Mostly, DWIBS alone can stage lymphoma according to Ann Arbor staging [42].

This study reported excellent agreement for the different stages of lymphomas according to Lugano classification. Other studies added PET-CT, and the results showed good agreement between MRI and PET/CT, slightly better than the intra- and inter-reproducibility of PET/CT itself [40,41]. In addition to the excellent interobserver reproducibility of DWIBS in the staging of lymphoma in this study, lymphoma patients with lymph nodes in stages III and IV showed lower ADC values than for those in stages I and II. Some previous studies compared FDG PET/CT and WB-MRI, with a focus on DWI, and they showed promising results, but these studies were considered exploratory. The accuracy of whole-body MRI with diffusion-weighted imaging was compared to contrast-enhanced CT and FDG PET in the staging of aggressive lymphoma, and it was concluded that WB MRI with DWI was the most reliable tool for the evaluation of bone marrow and its use instead of contrast-enhanced CT in the staging of lymphoma was supported [38-42].

Regarding the reliability of DWI in lymphoma staging, there is a discrepancy among the previous studies. Some demonstrated an increased diagnostic accuracy using DWI [43], while others did not find an improvement in staging performance [41]. Furthermore, in patients with residual mass after treatment, DWI might be a useful tool

for response assessment, helping to predict treatment outcome, and to differentiate resistant from a non-resistant disease, especially in patients with poor or absent decrease of lesion size due to the development of fibrosis. Thus, another important application of WB-MRI could be the response assessment of FDG-negative lymphomas, with the possibility of replacing CT with WB-MRI, avoiding ionizing radiation exposure during follow-up [41].

In our study, nodal ADC values differed between aggressive and indolent lymphoma patients. In a recent study that investigated nodal characterization in paediatric Hodgkin lymphoma patients by whole-body MRI with measurement of ADC, the diseased lymph nodes had significantly lower ADC values than benign lymph nodes [10]. Other studies used ADC to differentiate between benign and malignant cervical lymph nodes that had significantly lower ADC [44]. Another study compared benign lymphadenopathy to metastatic lymphadenopathy from head and neck cancers and lymphomatous lymph nodes that had a significantly lower mean ADC value [45], while the differentiation between normal and diseased lymph nodes

was achieved by ADC (ROC/AUC of 0.67–0.74), although the performance of the ADC was not greater than nodal size [10].

The limitations of this study are, first, this study was performed upon patients with different subtypes of NHL, and further studies upon subtypes of NHLs are recommended. Second, image analysis was performed only for staging, and further studies for follow-up after therapy are recommended. Third, the study group was small; future studies on larger number of patients would be beneficial.

## Conclusions

DWIBS is a reliable and reproducible imaging modality for the detection, staging, and grading of nodal and extra-nodal involvement in patients with NHL. ADC can add further value in NHL staging and grading.

## Conflict of interest

The authors report no conflict of interest.

## References

- Lewis WD, Lilly S, Jones KL. Lymphoma: diagnosis and treatment. *Am Fam Physician* 2020; 101: 34-41.
- Buchbender C, Heusner TA, Lauenstein TC, et al. Oncologic PET/MRI, part 2: bone tumors, soft-tissue tumors, melanoma, and lymphoma. *J Nucl Med* 2012; 53: 1244-1252.
- Maggialetti N, Ferrari C, Minoia C, et al. Role of WB-MR/DWIBS compared to (18) F-FDG PET/CT in the therapy response assessment of lymphoma. *Radiol Med* 2016; 121: 132-143.
- Albano D, La Grutta L, Grasedonio E, et al. Pitfalls in whole body MRI with diffusion weighted imaging performed on patients with lymphoma: what radiologists should know. *Magn Reson Imaging* 2016; 34: 922-931.
- Albano D, Patti C, Lagalla R, et al. Whole-body MRI, FDG-PET/CT, and bone marrow biopsy, for the assessment of bone marrow involvement in patients with newly diagnosed lymphoma. *J Magn Reson Imaging* 2017; 45: 1082-1089.
- Razek AAKA, Shamaa S, Lattif MA, et al. Inter-observer agreement of whole-body computed tomography in staging and response assessment in lymphoma: the Lugano classification. *Pol J Radiol* 2017; 82: 441-447.
- Bezerra ROF, Recchimuzzi DZ, dos Santos Mota MM, et al. Whole-body magnetic resonance imaging in the oncology setting: an overview and update on recent advances. *J Comput Assist Tomogr* 2019; 43: 66-75.
- Kwee TC, Ludwig I, Uiterwaal CS, et al. ADC measurements in the evaluation of lymph nodes in patients with non-Hodgkin lymphoma: feasibility study. *MAGMA* 2011; 24: 1-8.
- De Paepe KN, De Keyzer F, Wolter P, et al. Improving lymph node characterization in staging malignant lymphoma using first-order ADC texture analysis from whole-body diffusion-weighted MRI. *J Magn Reson Imaging* 2018; 48: 897-906.
- Latifoltojari A, Punwani S, Lopes A, et al. Whole-body MRI for staging and interim response monitoring in paediatric and adolescent Hodgkin's lymphoma: a comparison with multi-modality reference standard including 18F-FDG-PET-CT. *Eur Radiol* 2019; 29: 202-212.
- Montoro J, Laszlo D, Zing NP, et al. Comparison of whole-body diffusion-weighted magnetic resonance and FDG-PET/CT in the assessment of Hodgkin's lymphoma for staging and treatment response. *Ecancelmedicalscience* 2014; 8: 429. doi: 10.3332/ecancer.2014.429.
- Albano D, Agnello F, Patti C, et al. Whole-body magnetic resonance imaging and FDG-PET/CT for lymphoma staging: assessment of patient experience. *Egypt J Radiol Nucl Med* 2017; 48: 1043-1047.
- Petralia G, Padhani AR. Whole-body magnetic resonance imaging in oncology: uses and indications. *Magn Reson Imaging Clin N Am* 2018; 26: 495-507.
- Razek AA, Tawfik A, Rahman MA, et al. Whole-body diffusion-weighted imaging with background body signal suppression in the detection of osseous and extra-osseous metastases. *Pol J Radiol* 2019; 84: e453-e458. doi: 10.5114/pjr.2019.90057.
- Vilanova JC, Garcia-Figueiras R, Luna A, et al. Update on whole-body MRI in musculoskeletal applications. *Semin Musculoskelet Radiol* 2019; 23: 312-323.
- Tunari N, Blackledge M, Messiou C, et al. What's new for clinical whole-body MRI (WB-MRI) in the 21<sup>st</sup> century. *Br J Radiol* 2020; 93: 20200562. doi: 10.1259/bjr.20200562.
- Albano D, Stecco A, Micci G, et al. Whole-body magnetic resonance imaging (WB-MRI) in oncology: an Italian survey. *Radiol Med* 2021; 126: 299-305.
- Petralia G, Koh DM, Attariwala R, et al. Oncologically Relevant Findings Reporting and Data System (ONCO-RADS): guidelines for the acquisition, interpretation, and reporting of whole-body MRI for cancer screening. *Radiology* 2021; 299: 494-507.

19. Hynes JP, Hughes N, Cunningham P, et al. Whole-body MRI of bone marrow: a review. *J Magn Reson Imaging* 2019; 50: 1687-1701.
20. Albano D, Bruno A, Patti C, et al. Whole-body magnetic resonance imaging (WB-MRI) in lymphoma: state of the art. *Hematol Oncol* 2020; 38: 12-21.
21. Zafar S, Sharma RK, Cunningham J, et al. Current and future best practice in imaging, staging, and response assessment for non-Hodgkin's lymphomas: the Specialist Integrated Haematological Malignancy Imaging Reporting (SIHMIR) paradigm shift. *Clin Radiol* 2021; 76: 391.e1-391.e18. doi: 10.1016/j.crad.2020.12.022.
22. Stéphane V, Samuel B, Vincent D, et al. Comparison of PET-CT and magnetic resonance diffusion weighted imaging with body suppression (DWIBS) for initial staging of malignant lymphomas. *Eur J Radiol* 2013; 82: 2011-2017.
23. Li S, Xue HD, Li J, et al. Application of whole body diffusion weighted MR imaging for diagnosis and staging of malignant lymphoma. *Chin Med Sci J* 2008; 23: 138-144.
24. Littooi AS, Kwee TC, de Keizer B, et al. Whole-body MRI-DWI for assessment of residual disease after completion of therapy in lymphoma: a prospective multicenter study. *J Magn Reson Imaging* 2015; 42: 1646-1655.
25. Meleshko AN, Kharuzhyk SA, Piatrouskaya NA. Response monitoring in follicular lymphoma by synchronous evaluation of minimal residual disease and diffusion-weighted MRI. *Exp Oncol* 2015; 37: 295-297.
26. Regacini R, Puchnick A, Shigueoka DC, et al. Whole-body diffusion-weighted magnetic resonance imaging versus FDG-PET/CT for initial lymphoma staging: systematic review on diagnostic test accuracy studies. *Sao Paulo Med J* 2015; 133: 141-150.
27. Toledano-Massiah S, Luciani A, Itti E, et al. Whole-body diffusion-weighted imaging in Hodgkin lymphoma and diffuse large B-cell lymphoma. *Radiographics* 2015; 35: 747-764.
28. Sun M, Cheng J, Zhang Y, et al. Application value of diffusion weighted whole body imaging with background body signal suppression in monitoring the response to treatment of bone marrow involvement in lymphoma. *J Magn Reson Imaging* 2016; 44: 1522-1529.
29. Azzedine B, Kahina MB, Dimitri P, et al. Whole-body diffusion-weighted MRI for staging lymphoma at 3.0T: comparative study with MR imaging at 1.5T. *Clin Imaging* 2015; 39: 104-109.
30. Kwee TC, Takahara T, Ochiai R, et al. Diffusion-weighted whole-body imaging with background body signal suppression (DWIBS): features and potential applications in oncology. *Eur Radiol* 2008; 18: 1937-1952.
31. Swerdlow SH, Campo E, Pileri SA, et al. The 2016 revision of the World Health Organization classification of lymphoid neoplasms. *Blood* 2016; 127: 2375-2390.
32. Cheson BD, Fisher RI, Barrington SF, et al. Recommendations for initial evaluation, staging, and response assessment of Hodgkin and non-Hodgkin lymphoma: the Lugano classification. *J Clin Oncol* 2014; 32: 3059-3068.
33. Cheson BD, Leonard JP. Monoclonal antibody therapy for B-cell non-Hodgkin's lymphoma. *N Engl J Med* 2008; 359: 613-626.
34. Stecco A, Romano G, Negru M, et al. Whole-body diffusion-weighted magnetic resonance imaging in the staging of oncological patients: comparison with positron emission tomography computed tomography (PET-CT) in a pilot study. *Radiol Med* 2009; 114: 1-17.
35. Kalkmann J, Lauenstein T, Stattaus J. Whole-body diffusion-weighted imaging in oncology. Technical aspects and practical relevance. *Radiology* 2011; 51: 215-219.
36. Manenti G, Ciccio C, Squillaci E, et al. Role of combined DWIBS/3D-CE-T1w whole-body MRI in tumor staging: comparison with PET-CT. *Eur J Radiol* 2012; 81: 1917-1925.
37. Koh DM, Blackledge M, Padhani AR, et al. Whole-body diffusion weighted MRI: tips, tricks, and pitfalls. *AJR Am J Roentgenol* 2012; 199: 252-262.
38. Balbo-Mussetto A, Cirillo S, Bruna R, et al. Whole-body MRI with diffusion-weighted imaging: a valuable alternative to contrast-enhanced CT for initial staging of aggressive lymphoma. *Clin Radiol* 2016; 71: 271-279.
39. Kharuzhyk S, Zhavrid E, Dziuban A, et al. Comparison of whole-body MRI with diffusion-weighted imaging and PET/CT in lymphoma staging. *Eur Radiol* 2020; 30: 3915-3923.
40. Spijkers S, Littooi AS, Kwee TC, et al. Whole-body MRI versus an FDG-PET/CT-based reference standard for staging of paediatric Hodgkin lymphoma: a prospective multicentre study. *Eur Radiol* 2021; 31: 1494-1504.
41. Kwee TC, Vermoolen MA, Akkerman EA, et al. Whole-body MRI, including diffusion-weighted imaging, for staging lymphoma: comparison with CT in a prospective multicenter study. *J Magn Reson Imaging* 2014; 40: 26-36.
42. Lin C, Itti E, Luciani A, et al. Whole-body diffusion-weighted imaging in lymphoma. *Cancer Imaging* 2010; 10 Spec no A(1A): S172-S178. doi: 10.1102/1470-7330.2010.9029.
43. Gu J, Chan T, Zhang J, et al. Whole-body diffusion-weighted imaging: the added value to whole-body MRI at initial diagnosis of lymphoma. *Am J Roentgenol* 2011; 197: 384-391.
44. Perrone A, Guerrisi P, Izzo L, et al. Diffusion-weighted MRI in cervical lymph nodes: differentiation between benign and malignant lesions. *Eur J Radiol* 2011; 77: 281-286.
45. Ali TFT. Neck lymph nodes: characterization with diffusion-weighted MRI. *Egypt J Radiol Nucl Med* 2012; 43: 173-181.